IEEE Access
Multidisciplinary | Rapid Review | Open Access Journal

Received May 7, 2020, accepted May 26, 2020, date of publication June 17, 2020, date of current version June 29, 2020.

Digital Object Identifier 10.1109/ACCESS.2020.3003005

Predictive Flux Control for Induction Motor Drives With Modified Disturbance Observer for Improved Transient Response

MUHAMMAD ABBAS ABBASI[1,2], (Member, IEEE), ABDUL RASHID HUSAIN[1], (Member, IEEE), NIK RUMZI NIK IDRIS[1], (Senior Member, IEEE), WAQAS ANJUM[1,2], HUSSAIN BASSI[3,4], (Member, IEEE), AND MUHYADDIN JAMAL HOSIN RAWA[3,5], (Member, IEEE)

[1]School of Electrical Engineering, Universiti Teknologi Malaysia, Johor Bahru 81310, Malaysia
[2]Department of Electronic Engineering, Faculty of Engineering, The Islamia University of Bahawalpur, Bahawalpur 63100, Pakistan
[3]Center of Research Excellence in Renewable Energy and Power Systems, K. A. CARE Energy Research and Innovation Center, King Abdulaziz University, Jeddah 21589, Saudi Arabia
[4]Department of Electrical Engineering, Faculty of Engineering, King Abdulaziz University, Rabigh 25732, Saudi Arabia
[5]K. A. CARE Energy Research and Innovation Center, Department of Electrical and Computer Engineering, Faculty of Engineering, King Abdulaziz University, Jeddah 21589, Saudi Arabia

Corresponding author: Abdul Rashid Husain (abrashid@utm.my)

This work was supported by the UTM-Proton Future Drive Lab, Universiti Teknologi Malaysia (UTM), Skudai, Malaysia, for experimental facility and King Abdulaziz University, Jeddah, Saudi Arabia, and King Abdullah City for Atomic and Renewable Energy, Riyadh, Saudi Arabia, for financial support under Grant KCR-KFL-05-20.

ABSTRACT This paper proposes an extended model based predictive flux control (MPFC) with modified disturbance observer speed loop for induction motors. The main advantages of the proposed method are the improvement of load estimation, the suppression of current overshoot at step changes in reference speed and the removal of weighting factor in the newly formulated cost function. Weighting factor is removed by using extended reference transformation which translates reference torque, generated by the speed controller, into equivalent stator flux vector eliminating the challenging task of gain tuning at different points of operation. Then, the load torque is considered as an unknown disturbance and the accuracy of load estimation during speed jumps is improved by using a reduced order PI observer (ROPIO) with low-pass filter (LPF) for improved integration. The observer is combined with disturbance rejection based control to design a composite speed controller replacing conventional PI loop. The effectiveness of the proposed method is validated on a two-level three-phase inverter fed induction motor drive using dSpace DS1104 controller board. The dynamic response of the proposed method is compared to previously proposed disturbance observer based controller (DOBC) for predictive torque control method. The load estimation error of the proposed method at speed jumps is reduced by 66% while current surges are also suppressed effectively.

INDEX TERMS Disturbance observer based control, induction motor drive, predictive flux control, reference speed jumps, transient response, weighting factor removal.

I. INTRODUCTION

Model based predictive torque control (MPTC) is an emerging type of MPC for AC motor drives and recently it has received a tremendous attention by the research communities [1]. As compared to traditional control strategies for induction motor drives such as Field-Oriented Control (FOC) and Direct Torque Control (DTC), MPTC offers numerous advantages such as easier implementation, incorporation of multiple objectives in single cost function, optimization based solution and inclusion of system nonlinearities and constraints. Finite Control Set MPTC (FCS-MPTC) is the most common form of MPTC widely reported in recent literature [2], [3]. It has a simple structure and does not require a switching lookup table like in DTC. FCS-MPTC is an optimization based approach where a cost function,

The associate editor coordinating the review of this manuscript and approving it for publication was Chao Yang.

This work is licensed under a Creative Commons Attribution 4.0 License. For more information, see https://creativecommons.org/licenses/by/4.0/

consisting of a weighted sum of torque and flux errors, is defined to determine the optimal switching state of the inverter. In its most common form, the errors in cost function are between the reference values of torque and stator flux magnitude and their future values at the next sampling instant. However, other objectives can also be added into the cost function. The future values are predicted from the mathematical model of induction motor using all the admissible switching states. The switching state which generates minimum value of cost function is chosen and directly applied to the inverter. The inverter translates this state to the corresponding voltage vector (VV) and applies it to the motor terminals. A weighting factor is added to the cost function to maintain the level of regulation between torque and flux due to their differing units of measurement. A higher value of weighting factor puts more emphasis on flux regulation whereas a lower value indicates that torque regulation is being given priority. One of the main issues with FCS-MPTC is the tuning of weighting factor [4], [5] for satisfactory performance. Some solutions to overcome weighting factor design include ranking based multi-objective optimization [6] and online adaptation of weighting factor [7]. However, these solutions either cannot be extended to cost functions with increased number of objectives or suffer from parameter variations [4].

FCS-MPTC, like other conventional controllers, uses cascaded control structure with inner torque loop and outer speed loop [8]. The outer loop normally employs traditional PI controller for generating torque reference for the inner loop and regulating the motor speed. The inner loop is required to have a relatively faster dynamic response, as compared to outer loop, to follow the reference torque and ensure closed loop stability. In real time implementations, simple saturation blocks are used to limit the reference torque to ensure safety limits on motor currents [9]. However, the use of saturation blocks may result in larger current overshoots and longer settling times. Moreover, cascaded structure using PI controller may require re-tuning of controller gains under different operating conditions due to bandwidth and time constant mismatches. Other disadvantages include higher steady state error under model uncertainties and external disturbances. To overcome the limitations of cascade control in MPTC, the cascade-free MPTC schemes have been introduced in [10]–[12]. However, the cost function formulation and weighting factor design for these methods becomes challenging and optimization of multiple objectives with different time constants increases the computational complexity.

In spite of its good steady state performance, a PI controller exhibits loss of nominal performance under transient period in the presence of parameter variations and external disturbances. To improve the robustness of speed controller against such model uncertainties and disturbances, disturbance observer based control (DOBC) can be used to replace conventional PI control [13], [14]. A DOBC observer is designed and implemented in [15] for FCS-MPTC under parameter variations and load disturbances. External load changes and model uncertainties are lumped together in a single disturbance and speed equation is used to obtain the desired estimator. A similar approach is adapted for FCS model based predictive current control (FCS-MPCC) in [16]. Other methods for recovering nominal performance of the outer speed loop include integral sliding mode control (I-SMC) [17], PID control [18] and feedback linearization [19]. However, these methods suffer from various problems such as chattering in I-SMC, difficulty in practical implementation of D part in PID and complexity of the techniques as compared to the simple PI solutions for disturbance rejections such as reduced order PI observer. A novel DOBC-MPTC is presented in [20] which assumes load torque as an unknown disturbance and a reduced order PI observer (ROPIO) is designed based on the work reported in [21]. It is proven in [21] that although ROPIO is designed for disturbance rejection, it is also inherently robust to parameter variations, explicitly limiting the disturbances to load torque changes only. However, in all these DOBC-MPTC formulations, it is assumed that reference speed is differentiable at all times, hence ignoring the sudden speed jumps where derivative term becomes infinite. The differentiability condition restricts the reference speed to vary slowly to avoid large overshoots in stator currents. One way to avoid this restriction on reference speed and eliminate derivatives from the DOBC design is to redefine speed equation in new variables without derivatives [22]. However, the resulting DOBC is not convenient for real time implementations [9].

This paper proposes a modified MPTC without weighting factor and ROPIO based DOBC considering the reference speed jumps. Therefore, the proposed work not only suggests improvement in the outer speed loop but also to the inner loop. Reference transformation is introduced in [4] to eliminate weighting factor from the MPTC and the resulting control is called predictive flux control (PFC). In this work, a modified reference transformation — convenient for real time implementation — is used to formulate PFC for the inner loop. Similarly for outer loop, an ROPIO-DOBC recently introduced in [9] is employed with some modifications for improving the performance of speed control especially for speed reference jumps. The resulting FCS-MPFC is compared to previously introduced ROPIO-DOBC scheme without speed jumps. The superiority of the proposed scheme, in terms of disturbance rejection capability, load estimation at speed jumps and suppression of the resulted higher currents, is illustrated by the experimental results obtained on an induction motor drive using two-level three-phase inverter and dSpace DS1104 controller board. In comparison to this work, the previously introduced method [20] is implemented on a fixed frequency controller board which does not take into account the direct nature of MPTC and resulting variable switching frequency. On the other hand, the work in [9] is applied to Field-Oriented Control (FOC) and its study for direct control algorithms has not been carried out. Moreover, the practical implementation of proposed

ROPIO in [9] does not take into account the problems associated with integration. The novelty of this work lies in both loops of the cascaded FCS-MPTC of induction motors. For the inner torque loop the use of weighting-factor-free formulation of MPTC using modified reference transformation gets rid of weighting factor. This modified reference transformation merges two different angular calculations into a single computation by employing simple trigonometric identities and the Lagrange approximation. For the outer speed loop augmentation of the controller with modified ROPIO (M-ROPIO) contributes to the improvement of transient response at reference speed jumps. The speed jumps are part of the inherent design of the observer and a low-pass filter is used to avoid DC drift and other problems associated with practical implementation of pure integrator. The resulting MPFC scheme is weighting-factor free and works satisfactorily under sudden speed jumps and does not generate stator current surges.

The rest of the paper is organized as follows. Section II provides the dynamic model of the induction motor which is used in different implementation phases of MPTC and MPFC as well as speed control loop. Model based predictive torque and flux controls are outlined in section III with detailed mathematical descriptions and the features of proposed MPFC. Section IV briefly reviews ROPIO based DOBC for speed loop and the modified ROPIO suitable to handle the reference speed jumps is also covered. Selected simulation and experimental results for the proposed method are given in section V and VI. Section VII concludes the paper and references are provided at the end.

II. DYNAMIC MODEL OF IM

The state space model of induction motor in stationary reference frame can be described by the following mathematical relations [8]:

$$\boldsymbol{v_s} = R_s \boldsymbol{i_s} + \frac{d\boldsymbol{\psi_s}}{dt} \tag{1}$$

$$0 = R_r \boldsymbol{i_r} - j\omega \boldsymbol{\psi_r} + \frac{d\boldsymbol{\psi_r}}{dt} \tag{2}$$

$$\boldsymbol{\psi_s} = L_s \boldsymbol{i_s} + L_m \boldsymbol{i_r} \tag{3}$$

$$\boldsymbol{\psi_r} = L_r \boldsymbol{i_r} + L_m \boldsymbol{i_s} \tag{4}$$

$$T = 1.5p\Im\mathfrak{m}\left\{\overline{\boldsymbol{\psi}_s}\boldsymbol{i_s}\right\} = -1.5p\Im\mathfrak{m}\left\{\overline{\boldsymbol{\psi}_r}\boldsymbol{i_r}\right\} \tag{5}$$

$$J\frac{d\omega_m}{dt} = T_e - T_l \tag{6}$$

where $\boldsymbol{i_s}$, $\boldsymbol{v_s}$ and $\boldsymbol{\psi_s}$ are stator current, voltage and flux vectors; $\boldsymbol{i_r}$ and $\boldsymbol{\psi_r}$ are rotor current and flux vectors; T and T_l are electromagnetic and load torques; ω_m and ω are mechanical and electrical rotor speeds; R_s and R_r are stator and rotor resistances; L_s, L_r and L_m are stator, rotor and mutual inductance; J is moment of inertia; p is number of pole pairs; $\overline{\boldsymbol{\psi_r}}$ and $\overline{\boldsymbol{\psi_s}}$ are complex conjugates of rotor and stator flux vectors and $\Im\mathfrak{m}$ represents the imaginary part of the complex vector.

III. MODEL BASED PREDICTIVE TORQUE AND FLUX CONTROL

A. MODEL BASED PREDICTIVE TORQUE CONTROL (MPTC)

The conventional model based predictive torque control (MPTC) consists of three stages: (i) estimation of torque T and flux $\boldsymbol{\psi_s}$ using an observer (ii) prediction of flux, current and torque for next time interval i.e. $\boldsymbol{\psi_s}^p(k+1)$, $\boldsymbol{i_s}^p(k+1)$ and $T^p(k+1)$ (iii) selection of optimal voltage vector (VV) from admissible VVs i.e. $VV = \{V_0, V_1, \cdots V_7\}$ [8]. In this work, an LPF (Voltage Model) based estimator is used for flux and torque which can be described by following equations [23]:

$$\hat{\boldsymbol{\psi}}_{\boldsymbol{s}}(k) = a.\left\{\hat{\boldsymbol{\psi}}_{\boldsymbol{s}}(k-1) + T_s\left(\boldsymbol{v_s}(k) - R_s\boldsymbol{i_s}(k)\right)\right\} \tag{7}$$

$$\hat{T}(k) = \frac{3}{2}p\Im\mathfrak{m}\left\{\bar{\boldsymbol{\psi}}_{\boldsymbol{s}}(k)\,\boldsymbol{i_s}(k)\right\} \tag{8}$$

where $a = \frac{1}{1+T_s\omega_c}$, T_s is sampling time and sampling instants are marked as $k-1$ for previous instant, k for current instant and $k+1$ for next sampling instant respectively. The accuracy of flux and torque estimation is affected by the operating speed of the drive [23]. At low speeds, the VM performs poorly and estimations are not accurate [24]. However, model mismatching and low speed operation are not the focus of this work. Under medium and higher speeds, VM gives relatively accurate estimations of flux and torque [23]. Based on the state-space model of IM, the predictions can be made using the following relations [8]:

$$\boldsymbol{\psi_s}^p(k+1) = \hat{\boldsymbol{\psi}}_{\boldsymbol{s}}(k) + T_s\left(\boldsymbol{v_s}(k) - R_s\boldsymbol{i_s}(k)\right) \tag{9}$$

$$T^p(k+1) = \frac{3}{2}p\Im\mathfrak{m}\left\{\bar{\boldsymbol{\psi}}_{\boldsymbol{s}}^p(k+1)\,\boldsymbol{i_s}^p(k+1)\right\} \tag{10}$$

$$\boldsymbol{i_s}^p(k+1) = \left(1+\frac{T_s}{\tau_\sigma}\right)\boldsymbol{i_s}(k) + \frac{T_s}{R_\sigma(T_s+\tau_\sigma)}\left\{\left(\frac{k_r}{\tau_r} - jk_r\omega\right)\hat{\psi}_r(k) + \boldsymbol{v_s}(k)\right\} \tag{11}$$

The cost function for the selection of optimal VV is written as:

$$g = \left|T^*(k+1) - T^p(k+1)\right| + \lambda\left|\left|\psi_s^*(k+1)\right| - \left|\psi_s^p(k+1)\right|\right| \tag{12}$$

where superscript $*$ denotes the reference values and λ is weighting factor. However, the major drawbacks of this class of MPTC are:

- Higher computational effort is required for the selection of optimal VV. If additional objectives are included to the cost function or a higher level converter topology is used, computational burden increases exponentially.
- Weighting factor tuning is a challenging task to achieve satisfactory performance.

B. MODEL BASED PREDICTIVE FLUX CONTROL (MPFC)

To remove the weighting factor from MPTC, one of the solution is described in [4] where the concept proposed is

based on the reference transformation which translates torque reference into an equivalent flux reference. The resulting cost function only consists of flux errors effectively removing weighting factor and the resulting method is called model based predictive flux control (MPFC). The electromagnetic torque equation can be expressed as [8]:

$$\hat{T} = \frac{3}{2} p\eta L_m \left| \left(\boldsymbol{\psi_r} \times \hat{\boldsymbol{\psi}}_s \right) \right| = \frac{3}{2} p\eta L_m \left| \psi_r \right| \left| \hat{\psi}_s \right| \sin \hat{\theta}_{rs} \quad (13)$$

where $\eta = \frac{1}{L_s L_r - L_m^2}$ is a constant and $\hat{\theta}_{rs}$ is the angle between rotor flux vector $\boldsymbol{\psi_r}$ and estimated stator flux vector $\hat{\boldsymbol{\psi}}_s$. In polar form, the flux vectors can be expressed as: $\boldsymbol{\psi_r} = |\psi_r| \angle \theta_r$ and $\hat{\boldsymbol{\psi}}_{\boldsymbol{s}} = \left| \hat{\psi}_s \right| \angle \hat{\theta}_s$ whereas $\hat{\theta}_{rs} = \hat{\theta}_s - \theta_r$. If the rotor flux is known, then (13) at reference values can be written as:

$$T^* = \frac{3}{2} p\eta L_m \left| \left(\boldsymbol{\psi_r} \times \boldsymbol{\psi_s}^* \right) \right| = \frac{3}{2} p\eta L_m \left| \psi_r \right| \left| \psi_s^* \right| \sin \theta_{rs}^* \quad (14)$$

where $\boldsymbol{\psi_s}^* = \left| \psi_s^* \right| \angle \theta_s^*$ is the reference stator flux vector and $\theta_{rs}^* = \theta_s^* - \theta_r$ which can be calculated as:

$$\theta_{rs}^* = \arcsin \left(\frac{T^*}{\frac{3}{2} p\eta L_m \left| \psi_r \right| \left| \psi_s^* \right|} \right) \quad (15)$$

Once the angle θ_{rs}^* is determined from (15), the reference stator flux angle can be computed as $\theta_s^* = \theta_{rs}^* + \theta_r$ which will effectively translate reference torque T^* into equivalent reference flux vector $\boldsymbol{\psi_s^*}$. This is known as ''reference transformation (RT)'' and the resulting cost function can be written as:

$$g = \left| \boldsymbol{\psi_s}^* (k+1) - \boldsymbol{\psi_s}^p (k+1) \right| \quad (16)$$

Although reference transformation removes weighting factor from the MPTC formulation, it however requires additional computations for flux positions i.e. θ_r and θ_{rs}^*. Moreover, to implement two different trigonometric functions in hardware to determine these positions at each sampling instant will require additional hardware resources and add to the cost of the controller. To overcome these challenges, a modified reference transformation (M-RT) is proposed as follows.

The reference flux angle θ_s^* can be expressed as:

$$\theta_s^* = \arctan \left(\frac{\psi_{r\beta}}{\psi_{r\alpha}} \right) + \arcsin \left(\frac{T^*}{\frac{3}{2} p\eta L_m \left| \psi_r \right| \left| \psi_s^* \right|} \right) \quad (17)$$

$$\theta_s^* = \arctan \left(\frac{\psi_{r\beta}}{\psi_{r\alpha}} \right) + \arctan \left(\frac{T^*}{\sqrt{\left(\frac{3}{2} p\eta L_m \left| \psi_r \right| \left| \psi_s^* \right| \right)^2 - (T^*)^2}} \right) \quad (18)$$

$$\theta_s^* = \arctan (u) + \arctan (v) \quad (19)$$

$$\theta_s^* = \arctan \left(\frac{u+v}{1-uv} \right) \quad (20)$$

The expression in (20) is a direct way to compute reference flux position avoiding two different angle calculations. To further simplify the computation of arctan function the following 3-point Lagrange approximation is used [25]:

$$\arctan (y) \approx \frac{\pi}{4} y + 0.273 y \left(1 - |y| \right), -1 \leq y \leq 1 \quad (21)$$

The complete block diagram of MPFC based on modified reference transformation along with disturbance observer based (DOB) speed controller is shown in Fig. 1.

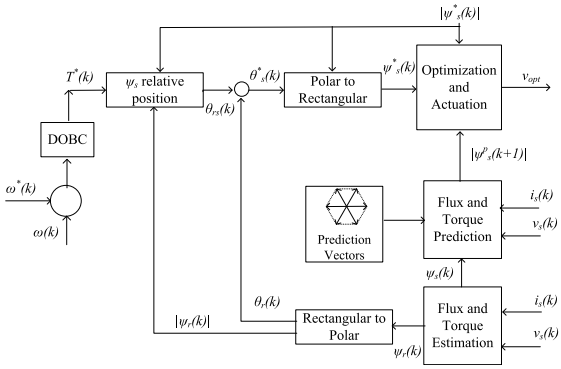

FIGURE 1. Predictive Flux Control (PFC) with Disturbance Observer based (DOB) Speed Controller.

IV. SPEED CONTROL WITH DISTURBANCE REJECTION

Most of the direct torque control (DTC) techniques use cascaded control structure where outer speed loop mainly serves to generate reference torque T^* for the inner loop. Ignoring frictional losses of the motor, the dynamic equation for speed loop can be written as (6). Using the same equation, reference torque T^* for MPFC can be written as:

$$T^* (t) = J \frac{d\omega_m (t)}{dt} + T_l (t) \quad (22)$$

where load torque T_l is considered an unknown disturbance and estimated using an observer. The PI based reduced order observer is used in this work due to its simplest configuration and capability to cope with external disturbance as well as parameter variations. There are other observers that are used such as adaptive observer, sliding mode observers and extended state observers [17], [26], [27]. However most of these methods require more complex design and demand higher computational time [28]. A simple predictive algorithm with prediction horizon T_p is proposed in [20] for speed tracking which allows the speed error e_ω to reach zero in single prediction step i.e.

$$\omega^* \left(t + T_p \right) - \omega_m \left(t + T_p \right) = 0 \quad (23)$$

where ω^* is the reference speed. Using the Taylor expansion, equation (IV) can be expressed as:

$$\omega^* (t) + T_p \frac{d\omega^* (t)}{dt} - \omega_m (t) - T_p \frac{d\omega_m (t)}{dt} = 0 \quad (24)$$

and from (24), the derivative term of speed can be written as:

$$\frac{d\omega_m (t)}{dt} = \frac{d\omega^* (t)}{dt} + \frac{1}{T_p} \left(\omega^*(t) - \omega_m(t) \right) \quad (25)$$

Substituting (25) in (22), the reference torque can be calculated as:

$$T^*(t) = \frac{J}{T_p}\left(\omega^*(t) - \omega_m(t)\right) + J\frac{d\omega^*(t)}{dt} + T_l(t) \quad (26)$$

This equation is also used for estimating load torque $\hat{T}_l$ as shown in following subsection.

A. REDUCED ORDER PI OBSERVER (ROPIO) FOR LOAD TORQUE

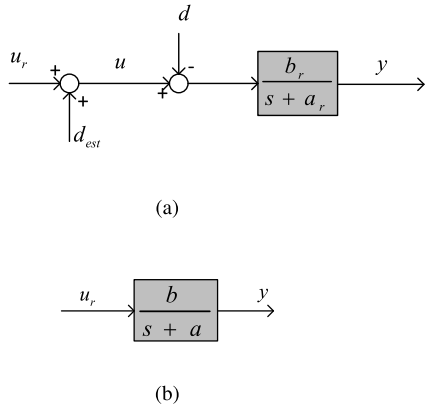

FIGURE 2. Disturbance observer based (DOB) speed control system [21] (a) Nominal System (b) Equivalent System.

If the bandwidth of speed loop is sufficiently smaller than the bandwidth of the inner torque loop, then speed loop can be approximated with a first order system shown in Fig. 2(*a*). The symbols used in the figure for IM drive application can be linked as: $d = T_l$ represents an unknown external disturbance, $u_r = T_e$ is the electromagnetic torque generated by the motor, $u = u_r + d_{est}$, $d_{est} = \hat{T}_l$ is the estimate of load torque, $b_r = \frac{1}{J}$, $a_r = \frac{B}{J}$ and $y = \omega_m$. The objective of this strategy is to design d_{est} in such a way that the output y from the system shown in Fig. 2(*a*) is equal to the output y of the system shown in Fig. 2(*b*). In this way, the estimate d_{est} should be as close as possible to d to cancel its effect. The system can be described by the following relation:

$$\dot{\omega}_m = -\frac{B}{J}\omega_m + \frac{1}{J}(T_e - T_l) \quad (27)$$

Assuming that system in Fig. 2(*a*) and in Fig. 2(*b*) produce exactly the same output and load torque is constant i.e. $\frac{dT_l}{dt} = 0$, the state space model of the system can be represented as:

$$\begin{bmatrix} \dot{\omega_m} \\ \dot{T_l} \end{bmatrix} = \begin{bmatrix} -\frac{B}{J} & -\frac{1}{J} \\ 0 & 0 \end{bmatrix} \begin{bmatrix} \omega_m \\ T_l \end{bmatrix} + \begin{bmatrix} \frac{1}{J} \\ 0 \end{bmatrix} T_e \quad (28)$$

Considering load torque T_l as an unknown disturbance, the reduced order observer for (6) can be defined as:

$$\frac{d\hat{T}_l}{dt} = l\left(T_l - \hat{T}_l\right) \quad (29)$$

where $\hat{T}_l$ is estimated load torque and l is observer gain. Combining (22) and (29), the corresponding ROPIO can be written as [21]:

$$\frac{d\hat{T}_l}{dt} = \frac{l}{J}\hat{T}_l(t) + l\left(\frac{d\omega_m(t)}{dt} - \frac{1}{J}T^*(t)\right) \quad (30)$$

Using the estimated load torque $\hat{T}_l$ in (26) and substituting the resulting equation back into (30):

$$\frac{d\hat{T}_l}{dt} = l\frac{d}{dt}\left(\omega^*(t) - \omega_m(t)\right) - \frac{l}{T_p}\left(\omega^*(t) - \omega_m(t)\right) \quad (31)$$

The load torque expression in (31) can be integrated to obtain the estimation of the unknown disturbance as,

$$\hat{T}_l = le_\omega(t) - \frac{l}{T_p}\int e_\omega(t)dt \quad (32)$$

where $e_\omega(t) = \omega^*(t) - \omega_m(t)$ is speed error at time instant t. It is clear from (32) that the observer behaves like a PI speed controller with disturbance rejection capability. From (26), however, it is evident that at reference speed jumps, the derivative term may cause high stator current surges to provide very large T^* and incorrect load estimates [9]. In the previous work [20], the reference speed is assumed to change slowly which may not be practical in many applications. To overcome this drawback, it can also be reformulated to avoid derivative terms as given in [21]. However, the resulted observer and controller are not convenient for real-time implementation.

B. MODIFIED ROPIO (M-ROPIO)

To minimize the effects of speed jumps, a modified load torque observer which is suitable for real time implementation is proposed in [9]. A similar observer with improvements is used in this work to remove the drawbacks of ROPIO and improve the accuracy of load estimation. The reference torque T^* generated by the speed loop may violate the bounds of the torque which motor can actually produce. Therefore, T^* is confined within the limits of rated torque of the motor T_{nom} to generate the effective reference torque given as:

$$T^*_{eff}(t) = \begin{cases} T_{nom} & , T^*(t) \geq T_{nom} \\ T^*(t) & , -T_{nom} < T^*(t) < T_{nom} \\ -T_{nom} & , T^*(t) \leq -T_{nom} \end{cases} \quad (33)$$

If the speed jumps occur at time instants $t_1, t_2, \ldots t_n$ and speed at starting time is defined as $\omega^*(0)$, then the reference speed for $t > t_i$ for $i = 1, 2, \ldots n$ can be written as:

$$\omega^*(t) = \omega^*(0) + \sum_{\tau=t_1}^{t_i} \Delta\omega^*(\tau) \quad (34)$$

where $\Delta\omega^*(t_i) = \omega^*(t_i) - \omega^*(t_i - T_{s\omega})$ are reference speed jumps and $T_{s\omega}$ is the sampling time of speed controller. Replacing the reference torque T^* in (30) with (33) and ignoring $\frac{d\omega^*(t)}{dt}$, the estimated load torque can be written as:

$$\frac{d\hat{T}_l}{dt} = l\frac{d\omega_m(t)}{dt} - \frac{l}{T_p}\left(\omega^*(t) - \omega_m(t)\right) + \frac{l}{J}\left(T^*(t) - T^*_{eff}(t)\right) \quad (35)$$

Let

$$\bar{T}(t) = \frac{l}{J}\int_0^t \left(T^*(t) - T^*_{eff}(t)\right) d\tau \tag{36}$$

Equation (36) in s domain can be written as:

$$\bar{T}(s) = \frac{l}{J}\frac{\left(T^*(s) - T^*_{eff}(s)\right)}{s} \tag{37}$$

To avoid the pure integration problems such as DC offset and drift in practical implementation of (37), an LPF with cutoff frequency ω_c can be used. The modified equation can be expressed as:

$$\bar{T}_{mod}(s) = \frac{l}{J}\frac{\left(T^*(s) - T^*_{eff}(s)\right)}{s + \omega_c} \tag{38}$$

which can be approximated by the following discrete-time relation:

$$\bar{T}_{mod}(k) = \frac{1}{1+\omega_c T_{s\omega}}\bar{T}_{mod}(k-1) + \frac{lT_{s\omega}}{J(1+\omega_c T_{s\omega})}(T^*(k) - T^*_{eff}(k)) \tag{39}$$

The approximation in above equation can be used to express the load estimation with speed jumps as:

$$\hat{T}_l(t) = -\frac{l}{T_p}\int_0^t e_\omega(t)d\tau - le_\omega(t) + \bar{T}_{mod}(t) + S(t) \tag{40}$$

where

$$S(t) = le_\omega(0) + l\sum_{\tau=t_1}^{t_i}\Delta\omega^*(\tau) \tag{41}$$

With these relations, a better load torque estimation is obtained especially at speed jumps which is not possible through basic ROPIO. If the load estimation is correct, it will lead to correct reference torque generation and avoid the current surges at sudden reference speed jumps as shown next in the experimental results.

V. SIMULATION RESULTS

In this section, selected simulation results are presented to validate the performance of M-ROPIO used with MPFC. The simulations are carried out in Matlab/Simulink environment with a sampling time of 40 μs. The three-phase induction motor drive model is used with the same parameters used for experimental results. The inverter, motor and observer models are built using discrete Simulink components whereas MPFC is implemented in a Matlab function block. The controller and motor parameters are given in Table 1 in next section.

To demonstrate the accuracy of (26) for reference torque (T^*) generation, simulations are carried out to compare the torque generated by (26) to the torque produced by standard reference torque generation method of PI controller. A step reference torque command is given to both PI controller and observer based on (26) and the generated T^* are shown in Fig. 3. The torque command is kept 0 $N.m.$ for $t < 2.2\ s$ and is stepped up to 4.7 $N.m.$ at $t = 2.2\ s$. It is evident from the figure that both the methods follow the torque command with (26) almost exactly copying the behavior of PI controller. Except for small deviations at start-up, it can safely be assumed that (26) is almost identical to PI method of reference torque generation with a comparable accuracy.

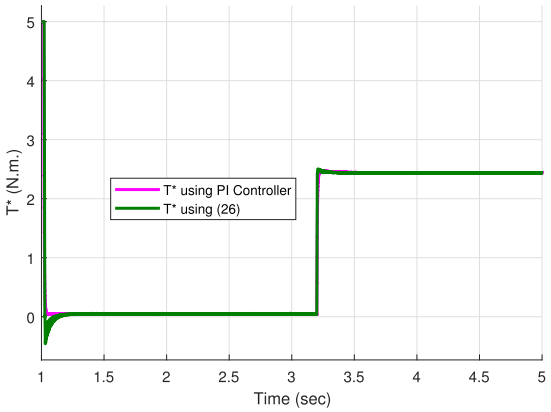

FIGURE 3. Comparison of reference torque (T^*) generation using PI controller and (26).

The disturbance rejection capabilities of ROPIO and M-ROPIO are demonstrated in Fig. 4 (*a*) and (*b*) respectively where motor torque T_e, speed ω, stator flux magnitude $\|\psi_s\|$ and estimated load torque T_l are shown from top to bottom for each observer. A load of 9.4 $N.m$ is applied at $t = 2.2\ s$ while maintaining the rated speed of 65 rad/s. It is clear from the figure that both the observers are able to reject the load disturbance and mainain the motor speed at the reference level. Whereas, these observers also provide the reasonable estimates of the load torque. A small decrease of 5 rad/s in motor speed is observed in both ROPIO and M-ROPIO at the application of disturbance which is quickly rejected by the observers. From these simulation results, it can be assumed that both ROPIO and M-ROPIO show similar disturbance rejection performance.

Although ROPIO and M-ROPIO show similar disturbance rejection and estimation performance for smooth reference speed, however, the advantage of M-ROPIO over ROPIO can be emphasized from reference speed jump tests. For this purpose, two speed tests without any external disturbance are conducted in simulations and the results for ROPIO and M-ROPIO are shown in Fig. 5 (*a*), (*b*) and 6 (*a*), (*b*) respectively. In Fig. 5 reference speed ω^* is increased from 40 rad/s to 65 rad/s at $t = 2.4\ s$ and back to 40 rad/s at $t = 4.3\ s$. The rotor speed ω and load torque T_l estimation are shown in figure for ROPIO and M-ROPIO. It is obvious from Fig. 5 (*a*) that ROPIO provides incorrect disturbance estimates. The reason for these results is that speed jumps are not considered in ROPIO design which lead to loss of nominal performance momentarily. M-ROPIO, on the other hand, generates load estimates up to 80% reduction in estimate error as compared to ROPIO. The error in estimates is even greater for bigger speed jumps such as speed reversal case.

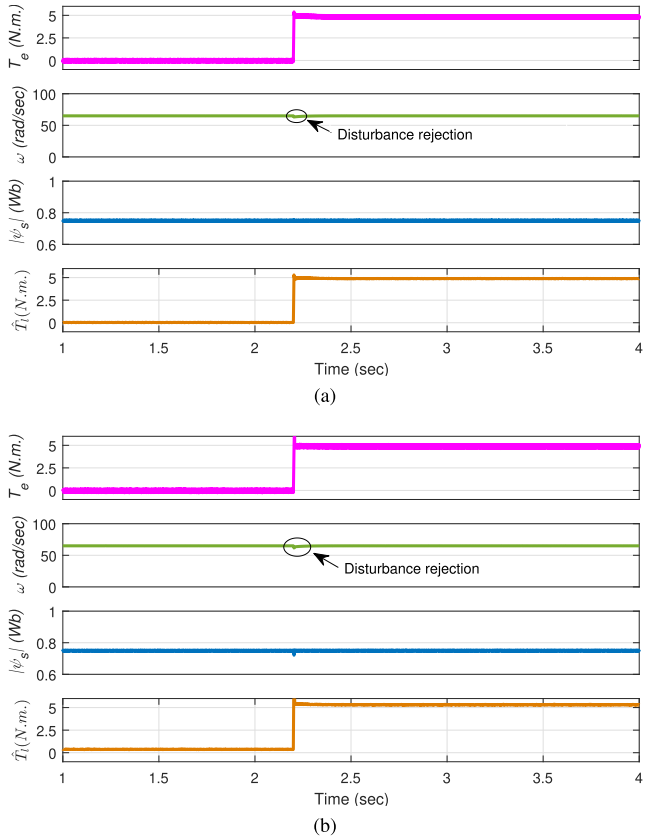

FIGURE 4. Simulation results for disturbance rejection capability of two observers used with MPFC for a step change in load torque (a) ROPIO (b) M-ROPIO.

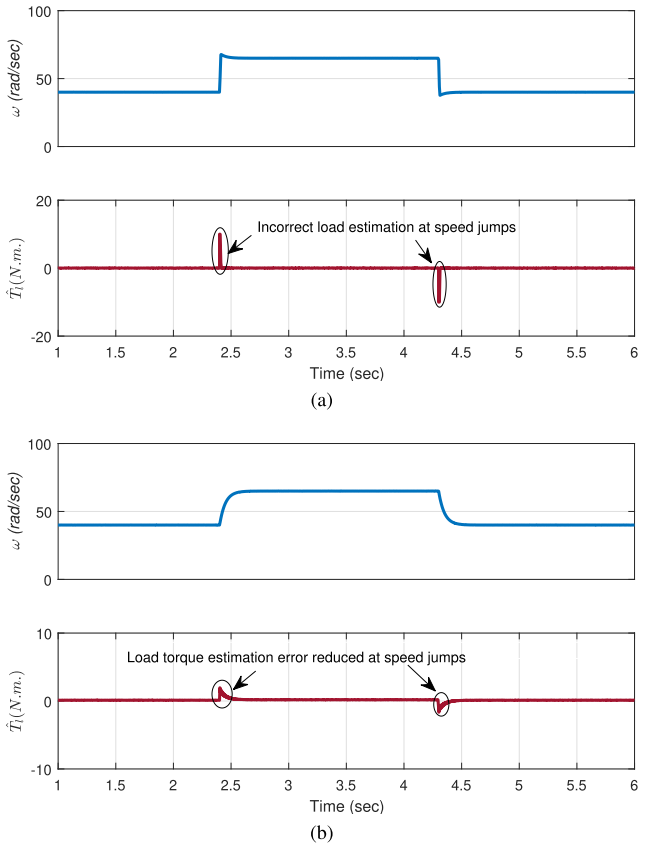

FIGURE 5. Simulation results for transient response of two observers used with MPFC for reference speed jumps (a) ROPIO (b) M-ROPIO.

In Fig. 6 (*a*) and (*b*), the disturbance estimation is shown for both ROPIO and M-ROPIO when reference speed is suddenly reversed from 65 rad/s to -65 rad/s at $t = 3.3$ s. For this case, ROPIO produces disturbance estimate errors which are 5 times larger than M-ROPIO estimate errors. Hence due to absence of reference speed jumps in inherent ROPIO design, its performance is inferior to M-ROPIO in terms of load disturbance estimation error.

The effect of wrong disturbance estimates on stator currents is shown in Fig. 7 where phase *a* current i_α waveform are shown for reference speed jump conditions. In this case, ROPIO produces current surges at the jump instants $t = 2.4$ s and $t = 4.3$ s. These current surges reach up to double of the steady state values of the current whereas M-ROPIO maintains the steady state value of current irrespective of the speed jumps.

VI. EXPERIMENTAL RESULTS

To investigate the effectiveness of proposed method, a 2L-VSI fed induction motor drive is used. The experimental setup, shown in Fig. 8, consists of 3 phase induction motor with hysteresis braking system, IGBT based inverter with a DC source and dSpace DS1104 controller board. The proposed control algorithm is implemented in dSpace using C coding. The optimal voltage vector selected by the algorithm is passed through an FPGA board which generates blanking time for the pulses to be applied to IGBTs through gate driver circuits. An incremental speed encoder with a resolution of 1024 pulses per revolution (PPR) and current sensors are also part of the setup to provide speed and current measurements respectively. The motor and controller parameters are given in Table 1. Note that same parameters were used in obtaining simulation results as well.

TABLE 1. Motor parameters.

Parameter	Value	Parameter	Value
Rated Torque,T_{nom}	10 $N.m.$	Stator Resistance, R_s	3 Ω
Rated Stator Flux, ψ_{s-nom}	0.75 Wb	Rotor Resistance, R_r	4.1 Ω
Base Speed, ω_{base}	65 rad/sec	Rotor Inductance, L_r	351 mH
Inverter DC source, V_{dc}	240 V	Mutual Inductance, L_m	324 mH
Total number of pole pairs, p	2	Total Inertia, J	0.0031 $kg.m^2$
Sampling Time, T_s	40 μs	Total viscous friction, B	0.0019 $kg.m^2/s$

During the practical implementation of the MPFC on dSpace DS1104, it was observed that average time to calculate inverse tangent function was around 2.73 μs. In original reference transformation, there are two positions to be determined for rotor flux vector and stator flux vector which requires an average time of 5.46 μs. With modified reference transformation, there is only one inverse tangent function

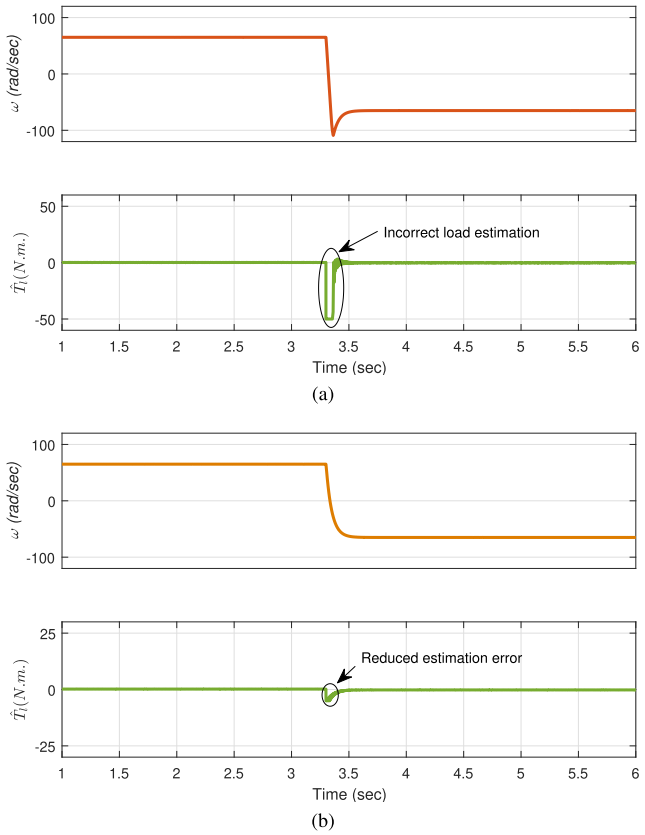

FIGURE 6. Simulation results for transient response of two observers used with MPFC under speed reversal condition (a) ROPIO (b) M-ROPIO.

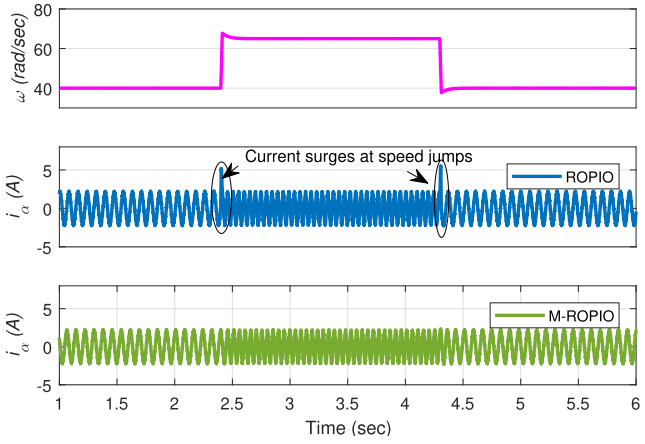

FIGURE 7. Effect of speed jumps on stator current (phase *a*) for two observers used with MPFC.

involved whereas with the use of Lagrange approximations the average computational time is reduced to 0.66 μs. Hence M-RT significantly reduces the computational time while keeping all the advantages of reference transformation. This reduction in computational time can be employed to use lower sampling times (T_s) for the controllers.

To emphasize the weighting-factor-less advantage achieved in MPFC through modified reference transformation,

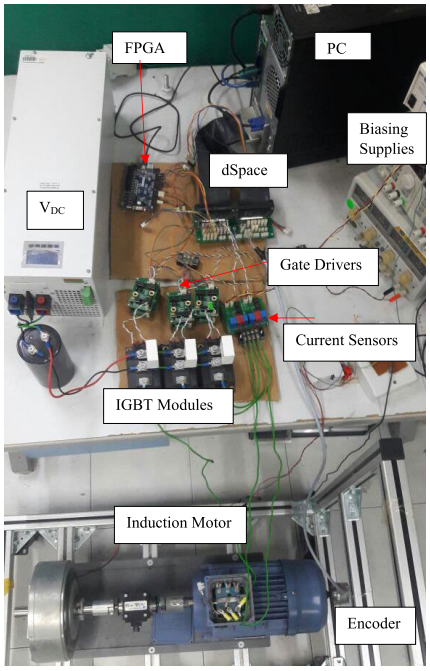

FIGURE 8. Actual hardware setup for real-time implementation of the proposed work.

the value of minimum costs of the objective functions of MPTC and MPFC under steady state operation are compared in Fig. 9. The minimum cost function for MPTC has larger values between 0 and 0.27 due to the fact that it consists of two differing errors i.e. torque and flux errors combined through a weighting factor. Wide variations in minimum cost can be reduced by adjusting weighting factor which will set a better balance between the two errors. Whereas, MPFC minimum cost function is almost zero (its actual value remains close to 0.005) due to the fact that it consists of only single error which achieves a better minimization.

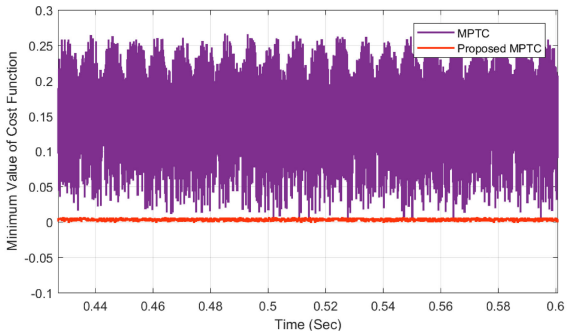

FIGURE 9. The values of the minimum costs obtained for MPTC and MPFC under steady state operation.

Similarly, the selection of the optimal VV at each sampling instant can also be compared for the two inner loop methods. Under steady state conditions, the optimal VV is plotted in Fig. 10 for MPTC and MPFC. For the very short interval of time shown in the figure, MPTC optimal vector could

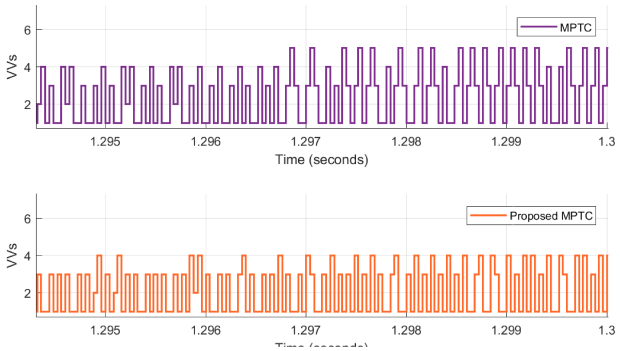

FIGURE 10. Optimal VV for MPTC and MPFC under steady state conditions.

be from V_1, V_2, V_3, V_4 and V_5 and there are sudden jumps from one VV to another which might not be the closest one. The pattern contributes to the higher switching frequencies. This pattern however is reduced in MPFC and switching states are from one VV to the neighboring VV which will not increase switching frequencies significantly. Moreover, number of total optimal VV selected for MPFC is less than MPTC. Keeping in mind the benefits of MPFC, the rest of the experimental results are obtained only for MPFC whereas similar results can be obtained for MPTC but with a larger flux and torque ripples.

Fig. 11 (*a*) and (*b*) demonstrates the disturbance rejection capability of both ROPIO and M-ROPIO when they are combined with MPFC. Similar to the simulation results presented in Fig. 4, a step change of 9.4 $N.m.$ in load torque is applied at $t = 2.2\ s$ to the motor when it is running at a constant reference speed of 65 rad/s. Waveform of estimated torque, speed, stator flux magnitude and estimated load torque are shown in the figure for both observers. It is clear from the speed response in Fig. 11 (*a*) that the load observer ROPIO not only correctly estimates the load torque but also rejects its effect on the speed regulation and removes steady state error quickly. At the disturbance load application, a reduction of 5 rad/sec in rotor speed is observed but it is overcome within 0.4 s and the speed is maintained at the given reference. Similarly, Fig. 11 (*b*) represents the steady state performance recovery response of the newly proposed M-ROPIO for the same test. As seen from rotor speed waveform for M-ROPIO, the disturbance rejection capability of the modified observer is similar to ROPIO. The disturbance is rejected within 0.4 s while maximum speed error is around 4 rad/s. However, a comparison of torque and flux response of the two observers, shows M-ROPIO has comparatively better flux response than MPFC with ROPIO. Similarly torque ripple in ROPIO is around 1 $N.m.$ while in M-ROPIO, it is equal to 0.8 $N.m.$ (20% less).

Although, ROPIO works relatively satisfactory during steady state condition and demonstrates effective error rejection, its transient response at reference speed jumps and reversal conditions gives incorrect estimation of the load.

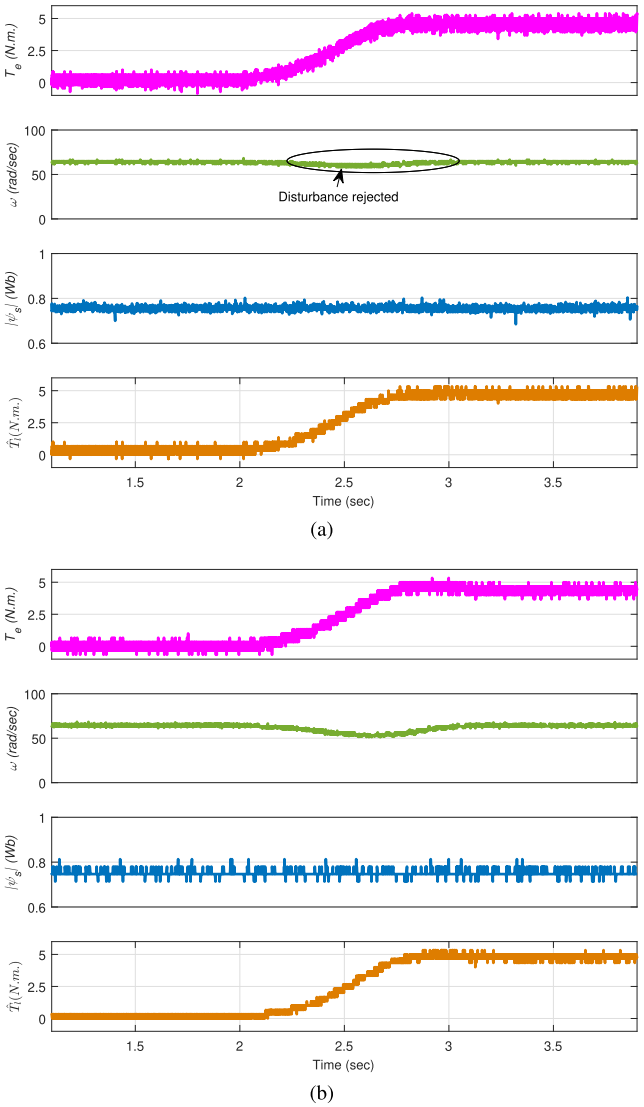

FIGURE 11. Experimental results for disturbance rejection capability of two observers used with MPFC for a step change in load torque (a) ROPIO (b) M-ROPIO.

Fig. 12 (*a*), (*b*) and 13 (*a*) and (*b*) represent experimental validation of simulation results obtained in Fig. 5 and 6 and show the rotor speed and estimated load torque for ROPIO and M-ROPIO under two different reference speed conditions. In Fig. 12, step changes in reference speed are applied to the unloaded motor and actual rotor speed and estimated load torque waveform are given for ROPIO and M-ROPIO. As shown in these waveform, reference speed changes from 40 rad/s to 65 rad/s at 2.4 s and back to 40 rad/s at 4.3 s. During these speed jumps, ROPIO scheme loses its performance momentarily and recovers from the loss within 0.1 s as shown in estimated load torque waveform. It happens because the reference speed jumps are ignored in the design. The error in load torque estimation for ROPIO is even greater when the jumps in reference

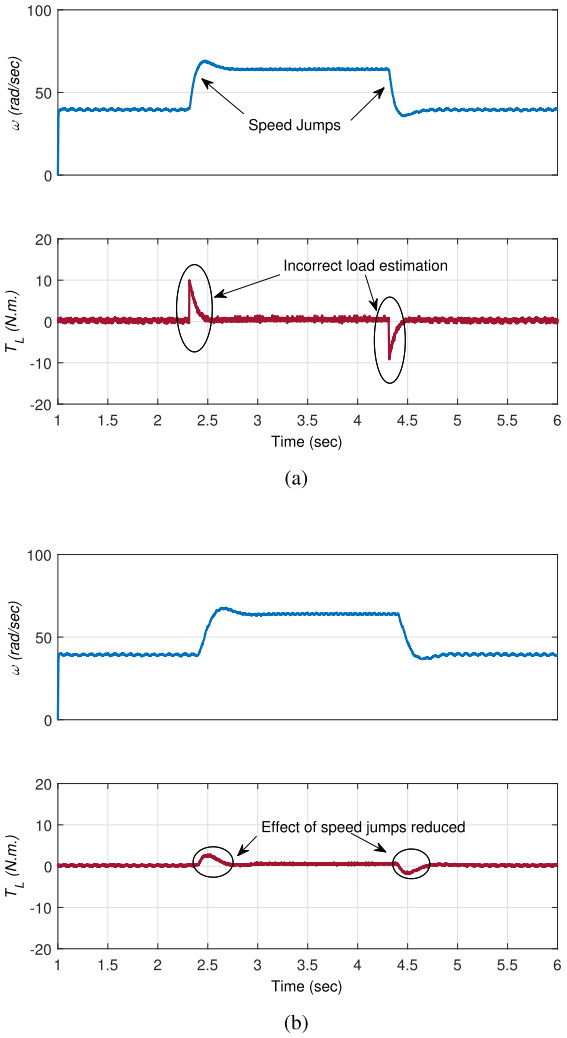

FIGURE 12. Transient response of two observers used with MPFC under speed jumps (a) ROPIO (b) M-ROPIO.

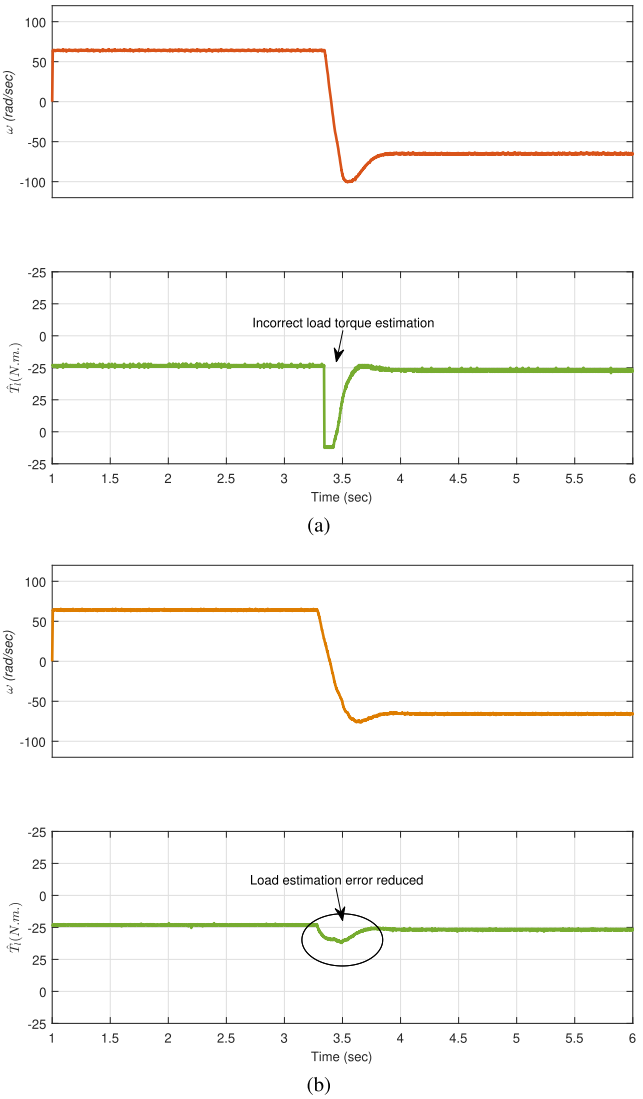

FIGURE 13. Transient response of two observers used with MPFC under speed reversal condition (a) ROPIO (b) M-ROPIO.

speed are larger as might be the case in speed reversal tests. The waveform of speed and estimated load torque for speed reversal test for ROPIO are shown in Fig. 13 (*a*). At time 3.3 *s*, reference speed is changed from 65 rad/s to -65 rad/s and the estimated torque by the load observer is recorded. As can be seen from the figure, estimation of load torque is incorrect at speed jump. The load observer gives 0.4 $N.m.$ error for a speed jump of 1 rad/s. The superiority of the modified observer M-ROPIO is clearer during transient response. The speed jump test and speed reversal test responses of M-ROPIO are shown in Fig. 12 (*b*) and Fig. 13 (*b*). It is visible from the waveform that observer response has improved significantly. A comparison of ROPIO and M-ROPIO responses reveals that error in load estimation has decreased close to 80% in M-ROPIO.

The phase *a* current waveform i_α comparison for both observers at sudden speed jumps is presented in Fig. 14. Stator current with proposed scheme M-ROPIO remains effectively smooth during short speed jump from 65 rad/s to 40 rad/s at $t = 2$ s, whereas, the same speed jump produces higher current for ROPIO and i_α deviates from the steady state value of maximum 1.8 A upto 3.3 A momentarily and quickly settles down to steady state value. However, this kind of short interval surges in current may be dangerous for safe motor operation.

To see the overall performance of both observers, an experiment combining reference speed reversal, speed jumps and a load was conducted. The motor starts unloaded at a reference speed of -65 rad/s. The reference speed is reversed to 40 rad/s around 1.8 s and increased to 65 rad/s around 3.8 s. A load of 5.2 $N.m.$ is applied around 5.5 s. The estimated load torque along with rotor speed are shown in Fig. 15 (*a*) and (*b*) for both observers ROPIO and M-ROPIO. It can be seen from the figure that modified observer gives better load torque estimation with significantly reduced error.

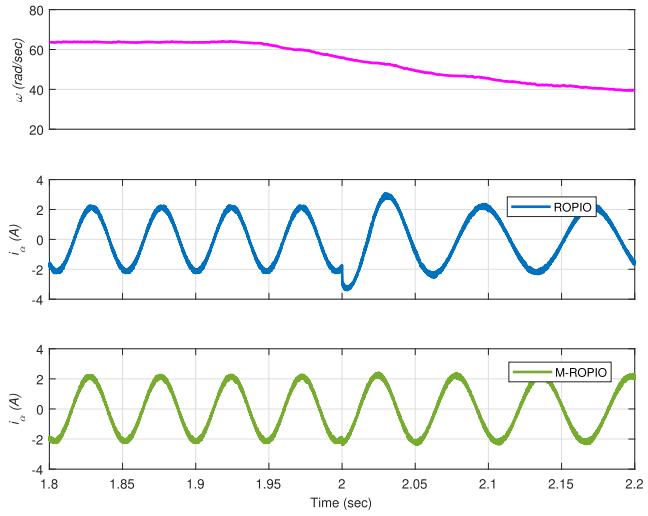

FIGURE 14. Comparison of stator currents (phase *a*) at speed jumps for ROPIO and M-ROPIO.

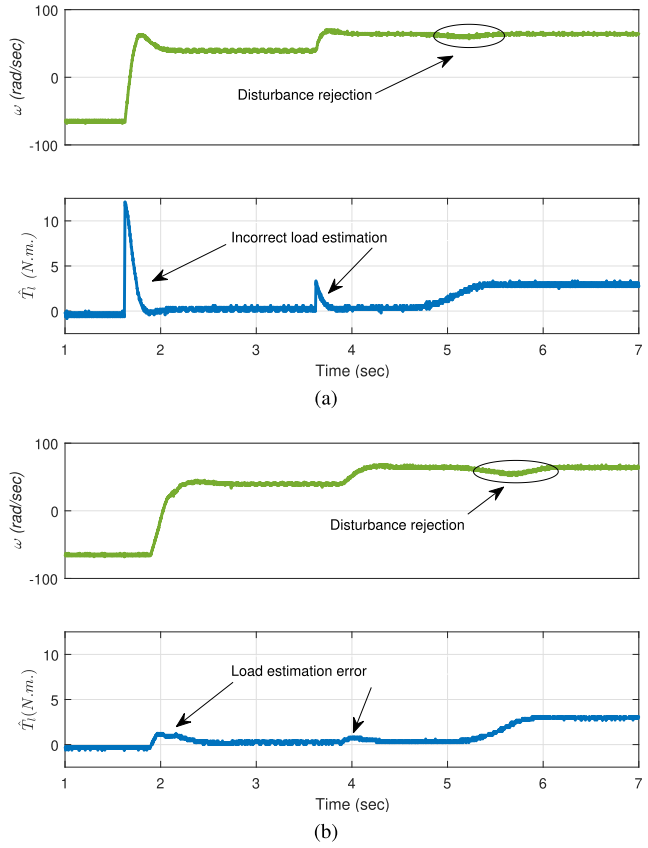

FIGURE 15. Transient response of two observers under speed jumps and load torque disturbance (a) ROPIO (b) M-ROPIO.

VII. CONCLUSION

A modified reference transformation is proposed to remove weighting factor from predictive torque control and a reduced order PI observer based disturbance rejection control (DOBC) is combined to improve transient response in this work. The resulting scheme shows superior performance as compared to the previously proposed method. The superiority of the proposed MPTC is demonstrated by lower load estimation error and effective current surge suppression at speed jumps while maintaining the comparable inner loop performance. Moreover, removal of weighting factor from the cost function gives an additional benefit of optimal balance between flux and torque regulation as evident from the simulation and experimental results.

REFERENCES

[1] S. Vazquez, J. Rodriguez, M. Rivera, L. G. Franquelo, and M. Norambuena, "Model predictive control for power converters and drives: Advances and trends," *IEEE Trans. Ind. Electron.*, vol. 64, no. 2, pp. 935–947, Feb. 2017.

[2] M. Habibullah, D. D.-C. Lu, D. Xiao, and M. F. Rahman, "A simplified finite-state predictive direct torque control for induction motor drive," *IEEE Trans. Ind. Electron.*, vol. 63, no. 6, pp. 3964–3975, Jun. 2016.

[3] W. Xie, X. Wang, F. Wang, W. Xu, R. M. Kennel, D. Gerling, and R. D. Lorenz, "Finite-Control-Set model predictive torque control with a deadbeat solution for PMSM drives," *IEEE Trans. Ind. Electron.*, vol. 62, no. 9, pp. 5402–5410, Sep. 2015.

[4] Y. Zhang, H. Yang, and B. Xia, "Model-predictive control of induction motor drives: Torque control versus flux control," *IEEE Trans. Ind. Appl.*, vol. 52, no. 5, pp. 4050–4060, Sep./Oct. 2016.

[5] A. Bhowate, M. Aware, and S. Sharma, "Predictive torque control with online weighting factor computation technique to improve performance of induction motor drive in low speed region," *IEEE Access*, vol. 7, pp. 42309–42321, 2019.

[6] C. A. Rojas, J. Rodriguez, F. Villarroel, J. R. Espinoza, C. A. Silva, and M. Trincado, "Predictive torque and flux control without weighting factors," *IEEE Trans. Ind. Electron.*, vol. 60, no. 2, pp. 681–690, Feb. 2013.

[7] S. A. Davari, D. A. Khaburi, and R. Kennel, "An improved FCS–MPC algorithm for an induction motor with an imposed optimized weighting factor," *IEEE Trans. Power Electron.*, vol. 27, no. 3, pp. 1540–1551, Mar. 2012.

[8] J. Rodriguez and P. Cortes, *Predictive Control of Power Converters and Electrical Drives*. Hoboken, NJ, USA: Wiley, 2012.

[9] R. Errouissi, A. Al-Durra, and S. M. Muyeen, "Experimental validation of a novel PI speed controller for AC motor drives with improved transient performances," *IEEE Trans. Control Syst. Technol.*, vol. 26, no. 4, pp. 1414–1421, Jul. 2018.

[10] M. Preindl and S. Bolognani, "Model predictive direct speed control with finite control set of PMSM drive systems," *IEEE Trans. Power Electron.*, vol. 28, no. 2, pp. 1007–1015, Feb. 2013.

[11] E. Fuentes, D. Kalise, J. Rodriguez, and R. M. Kennel, "Cascade-free predictive speed control for electrical drives," *IEEE Trans. Ind. Electron.*, vol. 61, no. 5, pp. 2176–2184, May 2014.

[12] A. Formentini, A. Trentin, M. Marchesoni, P. Zanchetta, and P. Wheeler, "Speed finite control set model predictive control of a PMSM fed by matrix converter," *IEEE Trans. Ind. Electron.*, vol. 62, no. 11, pp. 6786–6796, Nov. 2015.

[13] S. Li and J. Li, "Output predictor-based active disturbance rejection control for a wind energy conversion system with PMSG," *IEEE Access*, vol. 5, pp. 5205–5214, 2017.

[14] C. Jia, X. Wang, Y. Liang, and K. Zhou, "Robust current controller for IPMSM drives based on explicit model predictive control with online disturbance observer," *IEEE Access*, vol. 7, pp. 45898–45910, 2019.

[15] J. Wang, F. Wang, Z. Zhang, S. Li, and J. Rodriguez, "Design and implementation of disturbance compensation-based enhanced robust finite control set predictive torque control for induction motor systems," *IEEE Trans. Ind. Informat.*, vol. 13, no. 5, pp. 2645–2656, Oct. 2017.

[16] J. Wang, F. Wang, G. Wang, S. Li, and L. Yu, "Generalized proportional integral observer based robust finite control set predictive current control for induction motor systems with time-varying disturbances," *IEEE Trans. Ind. Informat.*, vol. 14, no. 9, pp. 4159–4168, Sep. 2018.

[17] M. Rubagotti, A. Estrada, F. Castanos, A. Ferrara, and L. Fridman, "Integral sliding mode control for nonlinear systems with matched and unmatched perturbations," *IEEE Trans. Autom. Control*, vol. 56, no. 11, pp. 2699–2704, Nov. 2011.

[18] T. Matsuo, R. Yoshino, H. Suemitsu, and K. Nakano, "Nominal performance recovery by PID+Q controller and its application to antisway control of crane lifter with visual feedback," *IEEE Trans. Control Syst. Technol.*, vol. 12, no. 1, pp. 156–166, Jan. 2004.

[19] A. A. Alfehaid, E. G. Strangas, and H. K. Khalil, "Speed control of permanent magnet synchronous motor using extended high-gain observer," in *Proc. Amer. Control Conf. (ACC)*, Jul. 2016, pp. 2205–2210.
[20] M. Ouhrouche, R. Errouissi, A. M. Trzynadlowski, K. Arab Tehrani, and A. Benzaioua, "A novel predictive direct torque controller for induction motor drives," *IEEE Trans. Ind. Electron.*, vol. 63, no. 8, pp. 5221–5230, Aug. 2016.
[21] Y. Ik Son, I. Hyuk Kim, D. Sik Choi, and H. Shim, "Robust cascade control of electric motor drives using dual reduced-order PI observer," *IEEE Trans. Ind. Electron.*, vol. 62, no. 6, pp. 3672–3682, Jun. 2015.
[22] J. Yang, W. X. Zheng, S. Li, B. Wu, and M. Cheng, "Design of a Prediction-Accuracy-Enhanced continuous-time MPC for disturbed systems via a disturbance observer," *IEEE Trans. Ind. Electron.*, vol. 62, no. 9, pp. 5807–5816, Sep. 2015.
[23] N. R. N. Idris and A. H. M. Yatim, "An improved stator flux estimation in steady-state operation for direct torque control of induction machines," *IEEE Trans. Ind. Appl.*, vol. 38, no. 1, pp. 110–116, Jan./Feb. 2002.
[24] I. M. Alsofyani and N. R. N. Idris, "A review on sensorless techniques for sustainable reliablity and efficient variable frequency drives of induction motors," *Renew. Sustain. Energy Rev.*, vol. 24, pp. 111–121, Aug. 2013.
[25] S. Rajan, S. Wang, R. Inkol, and A. Joyal, "Efficient approximations for the arctangent function," *IEEE Signal Process. Mag.*, vol. 23, no. 3, pp. 108–111, May 2006.
[26] H. Liu and S. Li, "Speed control for PMSM servo system using predictive functional control and extended state observer," *IEEE Trans. Ind. Electron.*, vol. 59, no. 2, pp. 1171–1183, Feb. 2012.
[27] J. S. Bang, H. Shim, S. K. Park, and J. H. Seo, "Robust tracking and vibration suppression for a two-inertia system by combining backstepping approach with disturbance observer," *IEEE Trans. Ind. Electron.*, vol. 57, no. 9, pp. 3197–3206, Sep. 2010.
[28] S. K. Kommuri, Y. C. Soh, J. J. Rath, M. Defoort, and K. C. Veluvolu, "Decoupled current control and sensor fault detection with second-order sliding mode for induction motor," *IET Control Theory Appl.*, vol. 9, no. 4, pp. 608–617, Feb. 2015.

MUHAMMAD ABBAS ABBASI (Member, IEEE) received the B.Sc. degree in electronics engineering from The Islamia University of Bahawalpur, Pakistan, in 2004, and the M.S. degree in electrical engineering from the University of Engineering & Technology (UET), Taxila, Pakistan, in 2012. He is currently pursuing the Ph.D. degree with Universiti Teknologi Malaysia (UTM). He has worked in different control industries in Pakistan. He has taught courses in control engineering, digital signal processing, FPGA based system design, and electronics systems. He is also a full-time Faculty Member with The Islamia University of Bahawalpur. His research interests include model predictive control of power converters and drives, predictive direct torque control, FPGA based control, and signal processing.

ABDUL RASHID HUSAIN (Member, IEEE) received the B.Sc. degree in electrical and computer engineering from The Ohio State University, Columbus, OH, USA, in 1997, the M.Sc. degree in mechatronics from the University of Newcastle Upon Tyne, U.K., in 2003, and the Ph.D. degree in electrical engineering (control) from Universiti Teknologi Malaysia (UTM), in 2009. Prior joining UTM, he worked as an Engineer in semiconductor industry specializing in precision molding and IC trimming process. His research interests include application of control in dynamic systems, robot navigation, mechatronic system design, and electrical drives and motion control. He is a member of IEEE Malaysia Chapter, Malaysia Simulation Society, and the Institute of Engineer Malaysia.

NIK RUMZI NIK IDRIS (Senior Member, IEEE) received the B.Eng. degree in electrical engineering from the University of Wollongong, Wollongong, NSW, Australia, in 1989, the M.Sc. degree in power electronics from Bradford University, West Yorkshire, U.K., in 1993, and the Ph.D. degree from Universiti Teknologi Malaysia (UTM), Johor Bahru, Malaysia, in 2000. He is currently an Associate Professor with UTM, and the Head of the Power Electronics and Drives Research Group. His current research interests include control of ac drive systems and DSP applications in power electronic systems. He is also the Past Chair of the Power Electronics Society, Malaysia Chapter.

WAQAS ANJUM received the B.Sc. degree in electronics engineering from The Islamia University of Bahawalpur, Pakistan, in 2007, and the M.S. degree in electrical engineering from the University of Engineering & Technology (UET), Taxila, Pakistan, in 2012. He is currently pursuing the Ph.D. degree with Universiti Teknologi Malaysia (UTM). He is also a full-time Faculty Member with The Islamia University of Bahawalpur. His research interests include modeling and control of power converters and observer design and optimization.

HUSSAIN BASSI (Member, IEEE) received the Ph.D. degree in electrical engineering from the University of Pittsburgh, in 2013. He is currently an Assistant Professor with the Department of Electrical Engineering, Faculty of Engineering, King Abdulaziz University, Rabigh. He is also attached to the Center of Research Excellence in Renewable Energy and Power Systems, K. A. CARE Energy Research and Innovation Center, King Abulaziz University, Jeddah. He contributes effectively to his discipline by adding innovative ideas and competes to add upon the state-of-the-art in power electronics technologies and renewable energy. He has ten pending and issued patents in renewable power and working on ten ongoing funded research projects with more than two million Saudi Riyals.

MUHYADDIN JAMAL HOSIN RAWA (Member, IEEE) was born in Makkah, Saudi Arabia, in August 1977. He received the B.Sc. degree in electrical and computer engineering from Umm Al-Qura University, in 2000, the M.Sc. degree in electrical and computer engineering, power and machines from King Abdulaziz University, in 2008, and the Ph.D. degree in electrical and electronic engineering from the University of Nottingham, in 2014. He has more than seven year's experiences in Saudi Electricity Company before joining the Department of Electrical and Computer Engineering, King Abdulaziz University, in 2008. He is currently the Deputy Director of the Center of Research Excellence in Renewable Energy and Power Systems. His research interests include power quality, renewable energy, and smart grids.